

General Disclaimer

One or more of the Following Statements may affect this Document

- This document has been reproduced from the best copy furnished by the organizational source. It is being released in the interest of making available as much information as possible.
- This document may contain data, which exceeds the sheet parameters. It was furnished in this condition by the organizational source and is the best copy available.
- This document may contain tone-on-tone or color graphs, charts and/or pictures, which have been reproduced in black and white.
- This document is paginated as submitted by the original source.
- Portions of this document are not fully legible due to the historical nature of some of the material. However, it is the best reproduction available from the original submission.

UNITED STATES
DEPARTMENT OF THE INTERIOR
GEOLOGICAL SURVEY

INTERAGENCY REPORT NASA-175

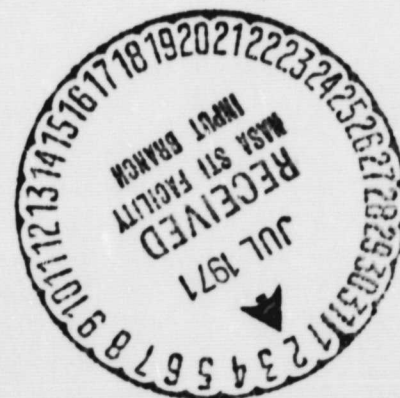
TEST OF DATA COMPILATION PROCEDURES FOR THE
FRAUNHOFER LINE DISCRIMINATOR

By

George E. Stoertz

1969

Prepared by the Geological Survey
for the National Aeronautics and
Space Administration (NASA)



Work performed under NASA Work Order No. T-80485C, Task 160-75-03-12-TA2511-TF41

U. S. Geological Survey, Washington, D. C.

FACILITY FORM 602

N71 - 332021

(ACCESSION NUMBER)

49

(PAGES)

CR 121427

(NASA CR OR TMX OR AD NUMBER)

(THRU)

G3

(CODE)

14

(CATEGORY)

NOTICE

On reproduction of this report, the quality of the illustrations may not be preserved. Full-size original copies of this report may be reviewed by the public at the libraries of the following U.S. Geological Survey locations:

**U.S. Geological Survey
1033 General Services Administration Bldg.
Washington DC 20242**

**U.S. Geological Survey
601 E. Cedar Avenue
Flagstaff, Arizona 86002**

**U.S. Geological Survey
345 Middlefield Road
Menlo Park, California 94025**

**U.S. Geological Survey
Bldg. 25, Denver Federal Center
Denver, Colorado 80225**

It is advisable to inquire concerning the timely availability of the original of this report and the possible utilization of local copying services before visiting a particular library.

There are no color illustrations in this report.

CONTENTS

Page

| | |
|--|----|
| Abstract | i |
| Introduction | 1 |
| Assumptions | 2 |
| Calculation of sunlight angles | 3 |
| Calculation of temperature correction factors | 4 |
| Calculation of total attenuation coefficients for emitted luminescence | 5 |
| Calculation of total attenuation coefficients for incident sunlight . | 9 |
| Calculation of attenuation by dye | 12 |
| Calculation of attenuation by turbidity | 15 |
| Calculation of sensitivity correction coefficients | 19 |
| Relation of sensitivity to solar intensity | 26 |
| Relation of FLD values to dye concentration | 27 |
| Summary and conclusions | 31 |
| References cited | 35 |

ILLUSTRATIONS

| <u>Figure</u> | <u>Follows page:</u> |
|---|--------------------------|
| 1. FLD recorder chart showing measurement of transmittance of yellow light by water samples, distilled water, and dye solutions . | 5 |
| 2. FLD recorder chart showing measurement of transmittance of green incident sunlight by water samples, distilled water, and dye solutions | 9 |
| 3. Relation between the ratio c_{te}/c_{ti} and the turbidity attenuation coefficient for yellow light (at 5890 Å) | 17 |
| 4. Relation of dye concentration to sensitivity correction coefficients between 12:14 and 12:20 p.m. on May 20, showing apparent exponential relationship | 24 |
| 5. Relation of sensitivity to solar intensity during airborne and shipboard tests of FLD | 27 |
| 6. Relation of sensitivity to solar intensity for four test areas . . . | 27 |
| 7. Graphical relations between dye concentration and FLD readings for short test periods | 30 |
| 8. Record from Fraunhofer Line Discriminator used as a shipboard fluorometer in San Francisco Bay, May 20, 1969 | 31 |
| 9. Record from Fraunhofer Line Discriminator used as an airborne fluorometer over Westpoint Slough, near Redwood Creek, southwest edge of San Francisco Bay, May 13, 1969 | 32 |
| 10. Record from Fraunhofer Line Discriminator used as an airborne fluorometer over San Francisco Bay, May 8, 1969 | 33 |
| 11. Record from Fraunhofer Line Discriminator used as an airborne fluorometer over Pacific Ocean west of Golden Gate, May 14, 1969 | 34 |

(ILLUSTRATIONS, continued)

| <u>Table</u> | <u>Page</u> |
|--|-------------|
| 1. Calculation of attenuation coefficients for emitted luminescence for water samples from San Francisco Bay | 7 |
| 2. Calculation of attenuation coefficients for incident light for water samples from San Francisco Bay | 10 |
| 3. Calculation of total attenuation coefficients of standard solutions of Rhodamine WT dye | 14 |
| 4. Relative attenuations of yellow light and green light by turbid San Francisco Bay waters | 16 |
| 5. Attenuation coefficients attributable to turbidity in San Francisco Bay and vicinity, showing relative consistence of the ratio c_{te}/c_{ti} | 18 |
| 6. Calculation of sensitivity correction coefficients for water samples from San Francisco Bay | 22 |
| 7. Calculation of relation between dye concentration and FLD readings for selected short test period | 29 |

ABSTRACT

Procedures for relating strip-chart records to fluorescent dye concentrations during operational use of the FLD over open water have been tested. It appears practicable to correct for the pertinent environmental and instrumental variables. FLD estimates of dye concentration require either frequent water sampling from the air, or frequent in-flight monitoring of standard targets. Procedures have been established for laboratory analysis of water samples and for compilation of the data. Compilation is tedious and will require use of a computer if the present FLD is extensively used for quantitative work. An improved model having only one photomultiplier should greatly reduce the variation in sensitivity and facilitate real-time data reduction. Use of any foreseeable model of FLD over relatively clear coastal waters or over ocean waters will require some sampling with depth. This has not yet been accomplished from the air and therefore related data compilation procedures have not yet been tested.

INTRODUCTION

The FLD integrates luminescence from a vertical column of dye solution approximately as deep as the penetration of green sunlight into the solution. Factors that are continuously variable in space and time are turbidity, water temperature, and dye concentration. These, in turn, result in continuous variations in depth of light penetration, attenuation of emitted luminescence, and attenuation of incident sunlight. Factors that vary in a less complicated way and are therefore more easily compensated, are sun angle and instrumental sensitivity.

It is difficult to correlate water samples obtained during airborne tests with FLD records because the recorder pen and the aircraft are both moving rapidly. If precise water-sample locations were possible, then FLD readings could be directly equated to dye concentrations by a direct empirical method.

However, frequent sampling is inconsistent with effective operational use of a remote sensor and would restrict the aircraft to such slow speeds that a boat might as well be used. During initial tests frequent water sampling served both as a substitute for the standard target device, and as a further check for theoretical calculations. The method of computation used in this report approximates the method that will be required in later operational use of the FLD, using the theoretical formulas that have been derived in previous reports (Stoertz, 1969).

ASSUMPTIONS

1) All of the samples containing rhodamine dye are surface samples, and it is assumed that the dye concentration in these samples extends uniformly throughout the column sensed by the FLD. Because of the exceedingly high turbidity of San Francisco Bay during the tests, the penetration of effective light must have averaged considerably less than one meter, and consequently this assumption probably does not introduce a significant error for tests over the Bay. This may not be the case, however, for tests over the Pacific Ocean.

2) Environmental conditions, especially turbidity, changed rapidly along the flight lines, and it was not possible to obtain samples representative of each change. Under these conditions it would be erroneous to weight the samples in proportion to their spacing. It was assumed that in a series of samples, each one should receive equal weight in determining average sensitivity, turbidity, and attenuation coefficients.

3) It was assumed that there is a linear relation between dye concentration and the attenuation coefficients (c_{di} and c_{de}) and between the dye concentration and instrumental sensitivity (S_c). This approximation enables solution of the theoretical formula relating dye concentration (R) to luminescence coefficient (ρ). As explained below it is probable that one or more of these are exponential functions, but if this linear approximation were not used, the formula could not be solved.

4) Attenuation coefficients attributable to water itself are assumed to be 0.14 m^{-1} for emitted yellow luminescence (c_{we}) and 0.05 m^{-1} for incident green sunlight (c_{wi}) (Stoertz, 1969). The remainder of calcu-

lated attenuation coefficients is attributed to turbidity, so the errors in these assumed values should be largely compensated by errors in turbidity attenuation coefficients.

5) About 80 samples were tested for attenuation of both yellow and green light; about 180 samples were tested for attenuation of yellow light only. Samples that were tested for both yellow and green attenuation had a fairly constant ratio between these factors for each test area. This approximation was used for estimating attenuation of green light in the remaining samples from each area.

CALCULATION OF SUNLIGHT ANGLES

Sun angles during airborne tests were determined from the American Ephemeris and Nautical Almanac. Times were noted in Pacific daylight saving time (7 hours behind GMT). The local time of sun's transit of the test site meridian is obtained from the Almanac or from the equation of time as shown by the analemma on many globes (Strahler, 1962, p. 88). The difference between time of transit and time of each sample gives the sun's longitude at time of sampling. The sun's declination (i.e., latitude) on the day of the test is given by the Almanac. This is subtracted from the latitude of the test site to obtain the angular difference in latitude. Using a stereonet (Nevin, 1949, p. 380) the angular differences in latitude and longitude of sun's position from those of the test site are converted into the resultant angular difference, equivalent to angle of the sun from the zenith. Subtracting from

90° gives the angle of the sun above the horizon (ϕ). Refracted angles of sunlight below the water surface (θ) are calculated from the relation:

$$\frac{\cos \phi}{\cos \theta} = n$$

in which the index of refraction of light in air with respect to water (n) is taken as approximately 1.333.

CALCULATION OF TEMPERATURE CORRECTION FACTORS

The temperature of water samples from the surface of test areas was periodically measured by thermometer immediately after sampling. The surface water temperature of San Francisco Bay appears to have been gradually increasing from 17.0°C. to 20.2°C. during a two-week test period (May 4 to May 20). Average daily temperature correction factors (t_c) to adjust rho values for decreasing luminescence of Rhodamine WT dye with increasing temperature were determined by graph (Stoertz, 1969, Fig. 5) as follows:

| | |
|--------|--------|
| May 4 | - 1.08 |
| May 8 | - 1.08 |
| May 13 | - 1.06 |
| May 14 | - 1.07 |
| May 19 | - 1.04 |
| May 20 | 0.99 |

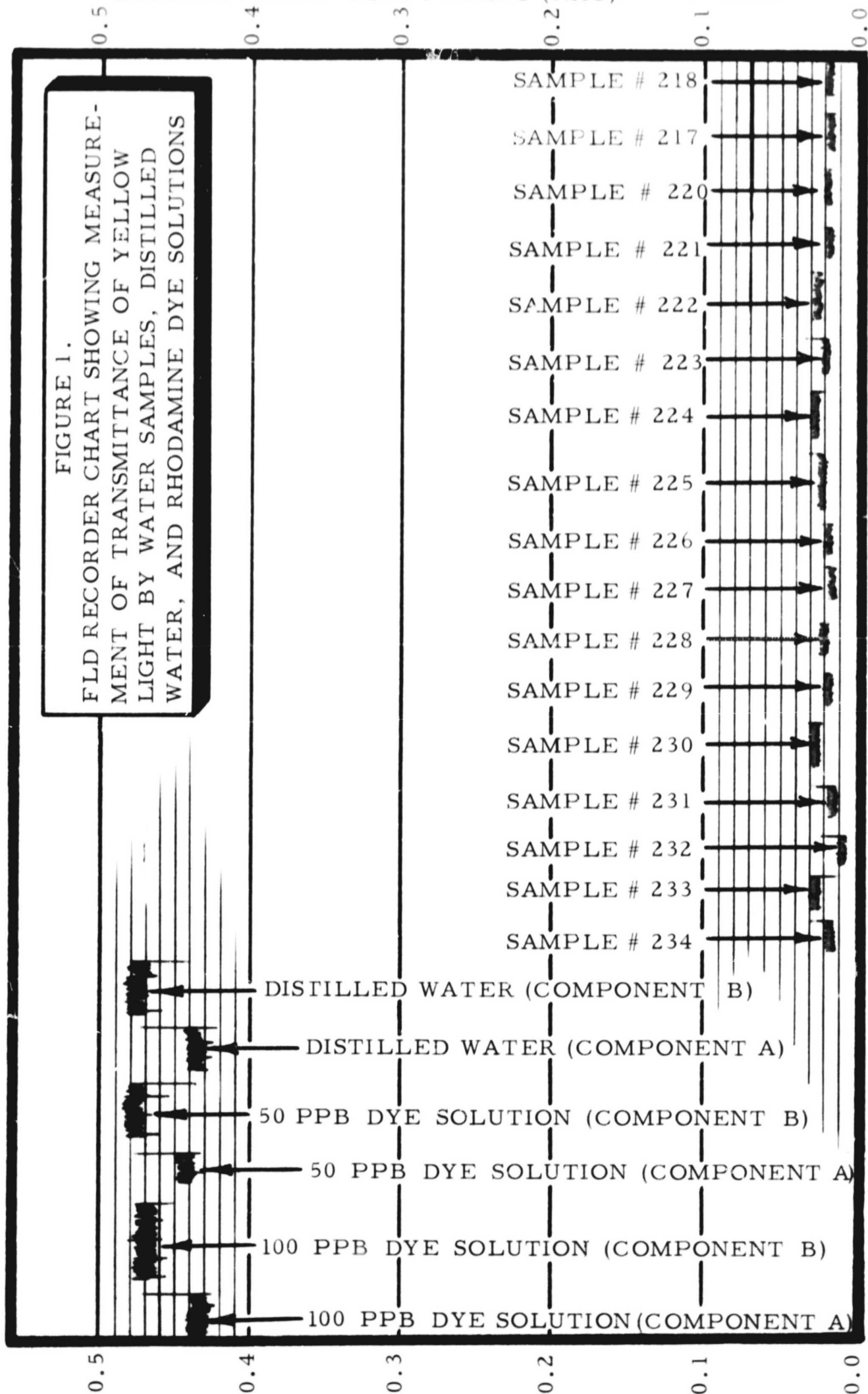
These factors are applied to adjust rho values for equivalence to a standard temperature of 20°C.

CALCULATION OF TOTAL ATTENUATION COEFFICIENTS FOR EMITTED LUMINESCENCE

A typical strip-chart record showing measurement of transmittance (T_e) of yellow light at 5890 Å by water samples, by distilled water, and by standard dye solutions is illustrated in Figure 1. For example, transmittances for samples #217 to #246 are shown by the series of short horizontal bars near the bottom of the chart, while the standards are shown by the heavier bars near the top. Sample transmittances are all measured in terms of component B. Transmittances of standards are measured in terms of both components A and B. It should be noted that B is somewhat higher than A in spite of illumination by artificial light, in which A (at 5892 Å) should be nearly identical to B (at 5890 Å). This apparently indicates a discrepancy between the gain of the two photomultipliers at the time of testing.

The higher values, appearing as heavier bars, illustrate the higher noise levels associated with higher light intensities. Transmittances of distilled water and of a 100-ppb dye solution are very close; this indicates that there is relatively little absorption or attenuation of yellow light (at 5890 Å) by Rhodamine WT dye. The very low transmittances of the water samples indicates that absorption of yellow luminescence by the dye is negligible in comparison with absorption by suspended particles.

The samples illustrated were all obtained on May 20 in San Francisco Bay south of San Mateo Bridge, and uniformity of most transmittances is evident, suggesting that sampling for turbidity during



FLD tests can be done at moderate intervals. Samples shown on Figure 1 were all taken from the POLARIS in shallow water and noticeable variations in turbidity were produced by the prop-wash. This may account for most of the variations evident on the chart.

The FLD readings (component B) on the chart are significant only in comparison to the readings for distilled water, the ratio of these values representing the transmittance of the sample in relation to that of distilled water. The equipment was not suitable for comparison of the transmittance of distilled water with that of air, due to internal reflections. This defect in the apparatus also increases the uncertainty in other values. The equipment has since been improved by use of less reflective materials, but some internal reflection undoubtedly still occurs. The error is probably not large for highly turbid samples, such as those from San Francisco Bay.

The method of calculating attenuation coefficients from these data is illustrated by a typical data sheet (Table 1) based on the same samples shown in Figure 1. This calculation uses the relation between transmittance (T) and attenuation coefficient (c) derived previously (Stoertz, 1969):

$$\log_e T = -cr \quad (\text{or}) \quad T = e^{-cr} \quad (1)$$

in which: T = Total transmittance: the ratio of the transmitted radiant flux to the incident radiant flux

e = 2.7183 . . . (Napierian base)

c = Total attenuation coefficient (m^{-1})

r = Path-length of the beam (meters)

Table 1. Calculation of attenuation coefficients for emitted luminescence for water samples from San Francisco Bay

(table includes same samples shown on Figure 1, obtained aboard POLARIS on May 20, south of San Mateo Bridge. Figures were rounded after the calculations were complete.)

| (1) | (2) | (3) | (4) | (5) | (6) | (7) | (8) |
|------------|---------|---------------|--|--|---|-----------------------|--|
| Sample no. | B_e^* | B_{we}^{**} | $\frac{B_e}{B_{we}} = \frac{(2)}{(3)}$ | $\frac{T_e \approx T_{we} B_e}{B_{we}} \approx 0.972 \times (4)$ | $\log T_e = \log (5)$ (-10 is omitted) | $-(\log T_e) = - (6)$ | $\frac{c_e = \frac{2.3026}{r} \log T_e}{(-\log T_e)} = 11.332 \cdot (7)$ (m^{-1}) |
| 217 | 0.012 | 0.475 | 0.025 | 0.024 | 8.386 | 1.614 | 18.3 |
| 218 | 0.018 | " | 0.038 | 0.037 | 8.568 | 1.432 | 16.2 |
| 219 | 0.017 | " | 0.036 | 0.035 | 8.544 | 1.456 | 16.5 |
| 220 | 0.019 | " | 0.040 | 0.039 | 8.590 | 1.410 | 16.0 |
| 221 | 0.018 | " | 0.038 | 0.037 | 8.568 | 1.432 | 16.2 |
| 222 | 0.027 | " | 0.057 | 0.055 | 8.744 | 1.256 | 14.2 |
| 223 | 0.022 | " | 0.046 | 0.045 | 8.650 | 1.350 | 15.3 |
| 224 | 0.028 | " | 0.059 | 0.057 | 8.759 | 1.241 | 14.1 |
| 225 | 0.023 | " | 0.048 | 0.047 | 8.669 | 1.331 | 15.1 |
| 226 | 0.018 | " | 0.038 | 0.037 | 8.568 | 1.432 | 16.2 |
| 227 | 0.016 | " | 0.034 | 0.033 | 8.519 | 1.481 | 16.8 |
| 228 | 0.022 | " | 0.046 | 0.045 | 8.650 | 1.350 | 15.3 |
| 229 | 0.019 | " | 0.040 | 0.039 | 8.590 | 1.410 | 16.0 |
| 230 | 0.028 | " | 0.059 | 0.057 | 8.759 | 1.241 | 14.1 |
| 231 | 0.017 | " | 0.036 | 0.035 | 8.544 | 1.456 | 16.5 |
| 232 | 0.009 | " | 0.019 | 0.018 | 8.266 | 1.734 | 19.6 |
| 233 | 0.027 | " | 0.057 | 0.055 | 8.744 | 1.256 | 14.2 |
| 234 | 0.017 | " | 0.036 | 0.035 | 8.544 | 1.456 | 16.5 |
| 235 | 0.016 | 0.465 | 0.034 | 0.033 | 8.519 | 1.481 | 16.8 |
| 236 | 0.014 | 0.465 | 0.030 | 0.029 | 8.465 | 1.535 | 17.4 |

* FLD-component "B" recorded for light (at 5890 Å) transmitted through sample.

** FLD-component "B" recorded for light (at 5890 Å) transmitted through distilled water.

Solving for transmittance of emitted light by distilled water (T_{we}) in the sample tube, the path-length (r) is known to be 0.203 meter and the attenuation coefficient for emitted luminescence (c_{we}) will be assumed to be approximately 0.14 m^{-1} (Stoertz, 1969, equation #25).

$$\begin{aligned}\therefore T_{we} &= e^{-c_{we}r} \\ &\cong 2.718^{-0.14 \cdot 0.203} \\ T_{we} &\cong 0.972\end{aligned}\tag{2}$$

With this apparatus the light intensity sensed through the upper portal of the FLD (component A or B) should be proportional to the transmittance, as defined above. Therefore, all samples should have approximately the same ratio between transmittances and recorded light intensities.

$$\therefore \frac{T_e}{B_e} \cong \frac{T_{we}}{B_{we}} \quad (\text{or}) \quad T_e \cong \frac{T_{we} B_e}{B_{we}}\tag{3}$$

in which: T_e = Transmittance of light (at 5890 Å) by a water sample

T_{we} = Transmittance of light (at 5890 Å) by distilled water

B_e = Recorded intensity of FLD-component B for light (at 5890 Å) transmitted through a water sample

B_{we} = Recorded intensity of FLD-component B for light (at 5890 Å) transmitted through distilled water

Application of equation (3) permits calculation of approximate transmittance of light (at 5890 Å) by the water samples (column #5 in Table 1). These values are for a path-length of only 20.3 cm. The corresponding total attenuation coefficients (c_e) for standard path-lengths of 1 meter are calculated by equation (1), as shown in the last 3 columns of Table 2:

$$\log_e T = -cr \quad (1)$$

$$(\text{or}) \log_e T_e = -c_e r$$

$$c_e = - \frac{\log_e T_e}{r}$$

$$c_e = - \frac{\log_e 10 \cdot \log T_e}{r}$$

in which: c_e = Total attenuation coefficient for light (at 5890 Å) by water sample

CALCULATION OF TOTAL ATTENUATION COEFFICIENTS FOR INCIDENT SUNLIGHT

Sections of a typical strip-chart record showing measurement of transmittance (T_i) of green light by water samples, by distilled water, and by standard dye solutions is illustrated in Figure 2. The samples illustrated include 10 of those shown on Figure 1. Apparatus used for the measurements has been described (Stoertz and others 1969). Transmittances of incident light through the samples are measured indirectly by means of the relative intensities of luminescence from a small cylinder of rhodamine dye excited by the incident light. Luminescence of the dye is recorded by means of rho. The lowest line on Figure 2 is a record of solar intensity (component A) measured at the upper portal, although in this case the FLD was lying on its side.

The marked fluctuations in rho values evident on Figure 2 result from gradual tilting of a hand-held mirror as it reflected sunlight through the sample tube. Only the maximum stable values are useful, representing the periods when sunlight was reflected exactly vertically into the vertical

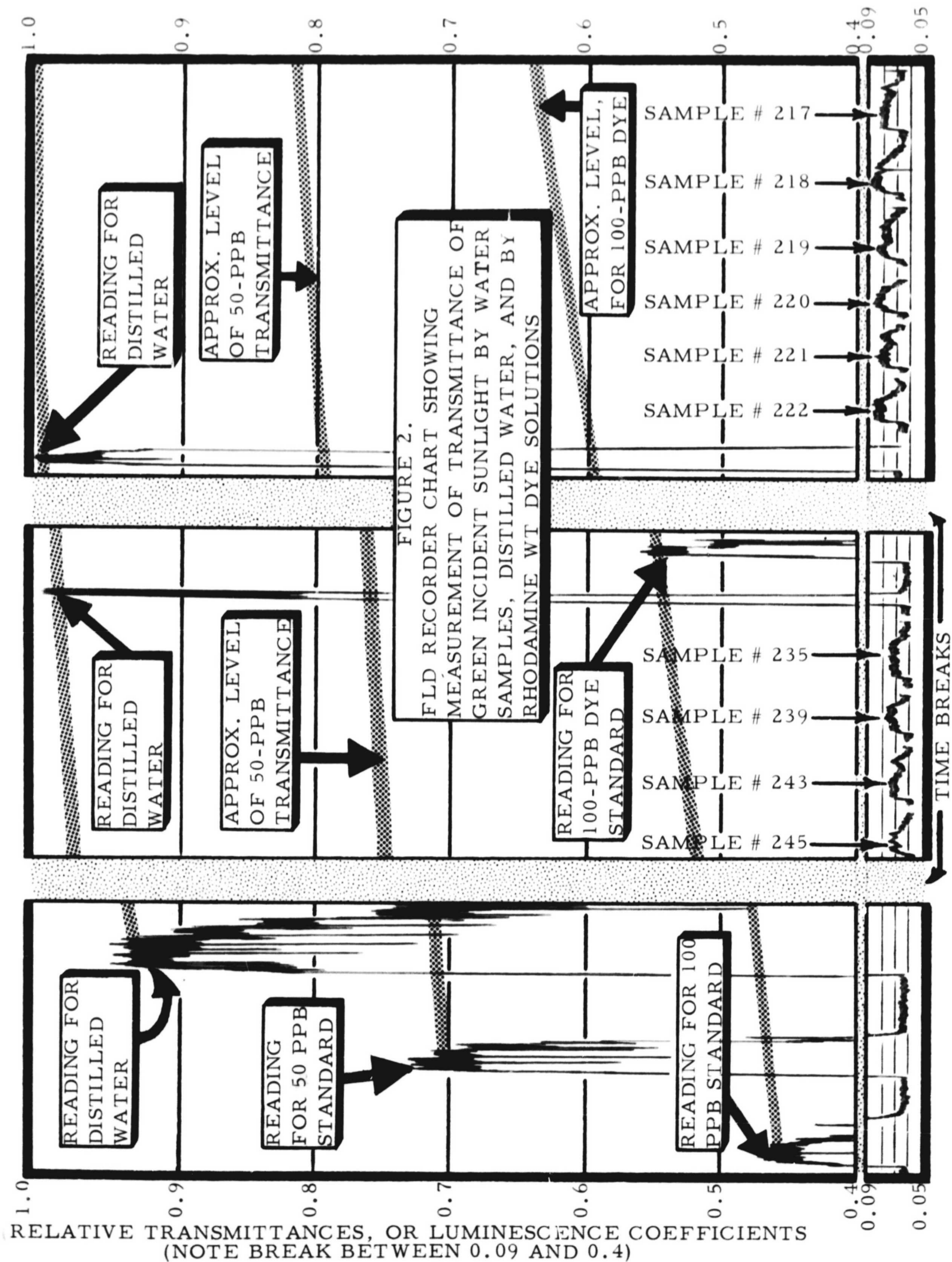


Table 2. Calculation of attenuation coefficients for incident light for water samples from San Francisco Bay

(table includes same samples shown on Figure 2, obtained aboard POLARIS on May 20. Figures were rounded after the calculations were complete.)

| (1) | (2) | (3)* | (4)* | (5) | (6) | (7) | (8) |
|------------|------------|----------------|--|--|---|----------------------|--|
| Sample no. | A_i^{**} | A_{wi}^{***} | $\frac{A_i}{A_{wi}} = \frac{(2)}{(3)}$ | $T_i \cong \frac{T_{wi} A_i}{A_{wi}} \cong 0.985 \times (4)$ | $\log T_i = \log (5)$ (-10 is omitted) | $-(\log T_i) = -(6)$ | $c_i = \frac{[\log_{e10} \log T_i]}{r} = \frac{2.3026}{0.297} \cdot (-\log T_i) = 7.753 \cdot (7)$ |
| 217 | 0.014 | 0.946 | 0.015 | 0.015 | 8.164 | 1.836 | 14.2 |
| 218 | 0.018 | 0.963 | 0.019 | 0.018 | 8.265 | 1.735 | 13.5 |
| 219 | 0.015 | 0.970 | 0.016 | 0.015 | 8.185 | 1.815 | 14.1 |
| 220 | 0.017 | 0.955 | 0.018 | 0.018 | 8.246 | 1.754 | 13.6 |
| 221 | 0.014 | 0.946 | 0.015 | 0.015 | 8.164 | 1.836 | 14.2 |
| 222 | 0.019 | 0.941 | 0.020 | 0.020 | 8.299 | 1.701 | 13.2 |
| 235 | 0.011 | 0.880 | 0.012 | 0.012 | 8.090 | 1.910 | 14.8 |
| 239 | 0.014 | 0.903 | 0.016 | 0.015 | 8.185 | 1.815 | 14.1 |
| 243 | 0.013 | 0.880 | 0.015 | 0.015 | 8.164 | 1.836 | 14.2 |
| 245 | 0.013 | 0.880 | 0.015 | 0.015 | 8.164 | 1.836 | 14.2 |

* Values were adjusted to correct for use of 50-ppb dye solution as a standard of comparison in lieu of distilled water, for which rho values were off scale.

** FLD-component "A" recorded for incident green light transmitted through sample .

*** FLD-component "A" recorded for incident green light transmitted through distilled water.

sample tube. Greater stability could be achieved by use of a mechanically operated mirror in a future model of the apparatus.

In this test, the values for dye solutions of 50 ppb and 100 ppb are markedly lower than those for distilled water, indicating a high rate of absorption of green light by Rhodamine WT dye. By comparison, absorption of green light by the suspended sediment of San Francisco Bay at the time of sampling (May 20) was evidently many times greater than that of a 100-ppb solution of rhodamine dye, as shown by the very low rho values for the samples. Samples shown were all obtained aboard the POLARIS in the area south of San Mateo Bridge.

As shown on Figure 2, the recorded rho value resulting from light transmitted through distilled water varied appreciably, apparently changing with sun angle. Frequently it went off the top of the scale (not shown). At such times it was necessary to use the value for a 50-ppb solution of rhodamine dye as a standard for comparison, instead of distilled water. A procedure similar to that described above (equations #1 to #3) was used. Attenuation coefficient of distilled water for incident green light (c_{wi}) has been estimated to be approximately 0.05 m^{-1} (Stoertz, 1969, equation #25). In this apparatus the path-length of light through the sample is 29.7 cm. (11.7 inches). Over this path-length the transmittance through distilled water (T_{wi}) is estimated to be approximately 0.985 m^{-1} .

The procedure used for computation of attenuation coefficients for the samples shown on Figure 2 is illustrated by a typical data sheet (Table 2),

using a method similar to Table 1 and equation (3):

$$\frac{T_i}{A_i} \cong \frac{T_{wi}}{A_{wi}} \quad (\text{or}) \quad T_i \cong \frac{T_{wi} A_i}{A_{wi}} \quad (4)$$

in which: T_i = Transmittance of incident green light by a water sample.

T_{wi} = Transmittance of incident green light by distilled water.

A_i = Recorded intensity of FLD-component A for incident green light transmitted through a water sample.

A_{wi} = Recorded intensity of FLD-component A for incident green light transmitted through distilled water.

CALCULATION OF ATTENUATION BY DYE

Procedures used for calculation of total attenuation coefficients (c_e and c_i) of water samples were described in the foregoing two sections. Interpretation of FLD readings (rho values) in terms of dye concentration requires that the component of total attenuation attributable to dissolved dye be separately evaluated and the relation expressed as a function of dye concentration. An estimate of this relation was previously based on the absorption spectrum of a known concentration of Rhodamine WT dye determined by spectrofluorometer (Stoertz, 1969). Results of recent attenuation tests also give data for estimating this relation, as described below. Because of the limitations of the apparatus, the results are considered an approximation. The results have been used in preliminary interpretation of FLD records.

Monitoring of 50-ppb and 100-ppb dye solutions during attenuation tests produced recorded values of light intensity (FLD-components A or B).

From this, total attenuation coefficients (c_e and c_i) were calculated by the same procedure used previously. Data are shown on Table 3.

The total attenuation coefficients must include components attributable to the dye (c_{de} and c_{di}) and to the water (c_{we} and c_{wi}). As stated previously, the latter values will be assumed to be 0.14 m^{-1} (c_{we}) and 0.05 m^{-1} (c_{wi}). Subtracting from total attenuation coefficients:

$$c_{de} = c_e - c_{we} ; c_{di} = c_i - c_{wi}$$

For 50 ppb: $c_{de} \cong 0.172 - 0.140 ; c_{di} \cong 0.800 - 0.050$

$$c_{de} \cong 0.032 (\text{m}^{-1}) ; c_{di} \cong 0.750 (\text{m}^{-1})$$

For 100 ppb: $c_{de} \cong 0.204 - 0.140 ; c_{di} \cong 1.512 - 0.050$

$$c_{de} \cong 0.064 (\text{m}^{-1}) ; c_{di} \cong 1.462 (\text{m}^{-1})$$

Relating the above coefficients to dye concentration (R):

$$\frac{c_{de}}{R} \cong \frac{0.032 \text{ m}^{-1}}{50 \text{ ppb}}$$

$$c_{de} \cong 0.00064 R \text{ m}^{-1} \quad (\text{average relation, 0 to 50 ppb})$$

$$\frac{c_{de}}{R} \cong \frac{0.064 \text{ m}^{-1}}{100 \text{ ppb}}$$

$$c_{de} \cong 0.00064 R \text{ m}^{-1} \quad (\text{average relation, 0 to 100 ppb})$$

$$\frac{c_{di}}{R} \cong \frac{0.750 \text{ m}^{-1}}{50 \text{ ppb}}$$

$$c_{di} \cong 0.015 R \text{ m}^{-1} \quad (\text{average relation, 0 to 50 ppb})$$

$$\frac{c_{di}}{R} \cong \frac{1.462 \text{ m}^{-1}}{100 \text{ ppb}}$$

$$c_{di} \cong 0.015 R \text{ m}^{-1} \quad (\text{average relation, 0 to 100 ppb})$$

Table 3. Calculation of total attenuation coefficients of standard solutions of Rhodamine WT dye

(figures were rounded after calculations were complete)

| (1) | (2) | (3) | (4) | (5) | (6) | (7) | (8) |
|---|-------------------|---------------|--|---|--|-----------------------|---|
| Standard solution of Rhodamine WT dye | B_e^* | B_{we}^{**} | Ratio: $\frac{B_e}{B_{we}} = \frac{(2)}{(3)}$ | $\frac{T_e B_{we} B_e}{B_{we}}$ $\cong 0.972 \times (4)$ (average values) | $\log T_e = \log (5)$ (- 10 is omitted) | $-(\log T_e) = - (6)$ | $c_e = \frac{[\log_{10} \log T_e]}{r}$ $= \frac{2.3026}{0.2032} \cdot (-\log T_e)$ $= 11.332 \cdot (7)$ (m^{-1}) |
| 50 ppb | 0.475 | 0.477 | 0.996 | | | | |
| | 0.463 | 0.467 | 0.991 | | | | |
| | Average (50 ppb) | | 0.9935 | 0.966 | 9.985 | 0.0152 | 0.172 |
| 100 ppb | 0.472 | 0.477 | 0.989 | | | | |
| | 0.460 | 0.467 | 0.985 | | | | |
| | Average (100 ppb) | | 0.987 | 0.959 | 9.982 | 0.0180 | 0.204 |
| Values below are for incident sunlight, calculated by same method | | | | | | | |
| Standards | A_i | A_{wi} | A_i/A_{wi} | T_i^{***} | $\log T_i$ | $-(\log T_i)$ | $c_i (m^{-1})$ |
| 50 ppb | 0.762 | 0.952 | 0.800 | 0.788 | 9.897 | 0.103 | 0.800 |
| 100 ppb | 0.617 | 0.952 | 0.648 | 0.638 | 9.805 | 0.195 | 1.512 |

* FLD-component "B" recorded for light transmitted through solution

** FLD-component "B" recorded for light transmitted through distilled water

*** $T_i \cong 0.985 \times 4$

Apparent values of constants for use in later formulas relating rho values to dye concentrations are:

$$\text{Let } c_{di} = f R ; \text{ Let } c_{de} = h R$$

$$c_{di} \approx 0.015 R \text{ m}^{-1} ; c_{de} \approx 0.00064 R \text{ m}^{-1}$$

$$\therefore f \approx 0.015 \text{ m}^{-1} ; h \approx 0.00064 \text{ m}^{-1}$$

CALCULATION OF ATTENUATION BY TURBIDITY

For purposes of interpreting FLD records, the term turbidity has been applied to all components of the water contributing to light attenuation other than dissolved rhodamine dye and the water itself. Therefore the attenuation coefficients due to turbidity (c_{te} and c_{ti}) include the combined effects of suspended sediment, organic matter, and coloring matter other than rhodamine dye. If the total attenuation coefficients (c_e and c_i) of a sample have been measured and the dye concentration (R) is known, the turbidity attenuation coefficients are determined as follows (all units are in m^{-1} except R , which is in ppb):

$$c_{te} = c_e - c_{we} - c_{de} ; c_{ti} = c_i - c_{wi} - c_{di}$$

$$\text{in which: } c_{de} = 0.00064 R ; c_{di} = 0.015 R$$

If either one of the total attenuation coefficients of a sample has been measured (e.g., c_e) an approximation of the other total attenuation coefficient (e.g., c_i) can be obtained, provided that a sufficient number of other samples from the same area have been tested. If other samples show a nearly consistent ratio between attenuation of yellow light by turbidity (c_{te}) and attenuation of green light by turbidity (c_{ti}) then the ratio (c_{te}/c_{ti}) can be applied to the untested samples. Samples from

Table 4. Relative attenuations of yellow light and green light by turbid San Francisco Bay waters

(based on 53 water samples from H-19 helicopter on May 8 and May 13, and from POLARIS on May 19 and May 20)

| Area sampled | No. of samples tested | Distribution of ratios c_{te}/c_{ti} by percent | | | | | | | | | Averages** | | |
|--|-----------------------|---|--------------|--------------|--------------|--------------|--------------|--------------|--------------|--------------|-------------------------------|-------------------------------|-------------------------------|
| | | 0.60 to 0.69 | 0.70 to 0.79 | 0.80 to 0.89 | 0.90 to 0.99 | 1.00 to 1.09 | 1.10 to 1.19 | 1.20 to 1.29 | 1.30 to 1.39 | 1.40 to 1.49 | Average ratio c_{te}/c_{ti} | Average c_{te} (m^{-1}) | Average c_{ti} (m^{-1}) |
| San Francisco Bay south of San Mateo Bridge (from the POLARIS) * | 30 | | | 3 | 3 | 20 | 17 | 17 | 17 | 10 | 1.24 | 17.5 | 14.1 |
| San Francisco Bay north of San Mateo Bridge (from the helicopter) | 4 | | 100 | | | | | | | | 0.76 | 7.53 | 9.92 |
| Westpoint Slough near Redwood Cr. southwest edge of S. F. Bay (fr. H-19) | 19 | 5 | 37 | 37 | 11 | | 5 | 5 | | | 0.83 | 8.14 | 9.93 |

* Samples from POLARIS show extraordinarily high turbidity attributable to disturbance of bottom sediments in shallow water by prop-wash.

**** Definitions:**

c_{te} - Attenuation coefficients attributable to suspended sediment, coloring matter (except dissolved fluorescent dye), and organic matter, for yellow light at 5890 Å. Intended to be applicable to attenuation of emitted luminescence at 5890 Å (units are reciprocal length, m^{-1})

c_{ti} - Attenuation coefficients attributable to suspended sediment, coloring matter (except dye) and organic matter for green incident sunlight in spectral range from about 5400 Å to about 5800 Å (units are reciprocal length, e.g., m^{-1})

San Francisco Bay had ratios falling predominantly within a small range for each test area (Table 4).

In general, it is concluded from the San Francisco Bay samples that the suspended particles in one area during the sampling period are likely to be sufficiently homogeneous that the ratio expressing relative attenuation of yellow light and green light will not vary significantly. At least the ratios were found to be more consistent than the absolute values of turbidity, which varied abruptly from place to place. The non-uniform distribution of turbidity was clearly visible from the air, the most turbid water having the appearance of long continuous strands of muddy water generally elongated in the direction of the current. The relative consistency of the ratios by contrast to the actual turbidity levels is shown by Table 5.

The figures on Tables 4 and 5 also show an apparent relation between the ratio (c_{te}/c_{ti}) and the actual levels of turbidity, as inferred from the attenuation coefficients (c_{te} and c_{ti}). This relation is shown graphically on Figure 3, based on tested samples from Westpoint Slough and from the area of San Francisco Bay south of San Mateo Bridge. It is evident from the graph that at the time of the tests, increases in turbidity were associated with larger increases in attenuation of yellow light in comparison with attenuation of green light.

Turbidity attenuation coefficients measured in samples from the Pacific Ocean were less consistent than in San Francisco Bay, the ratio

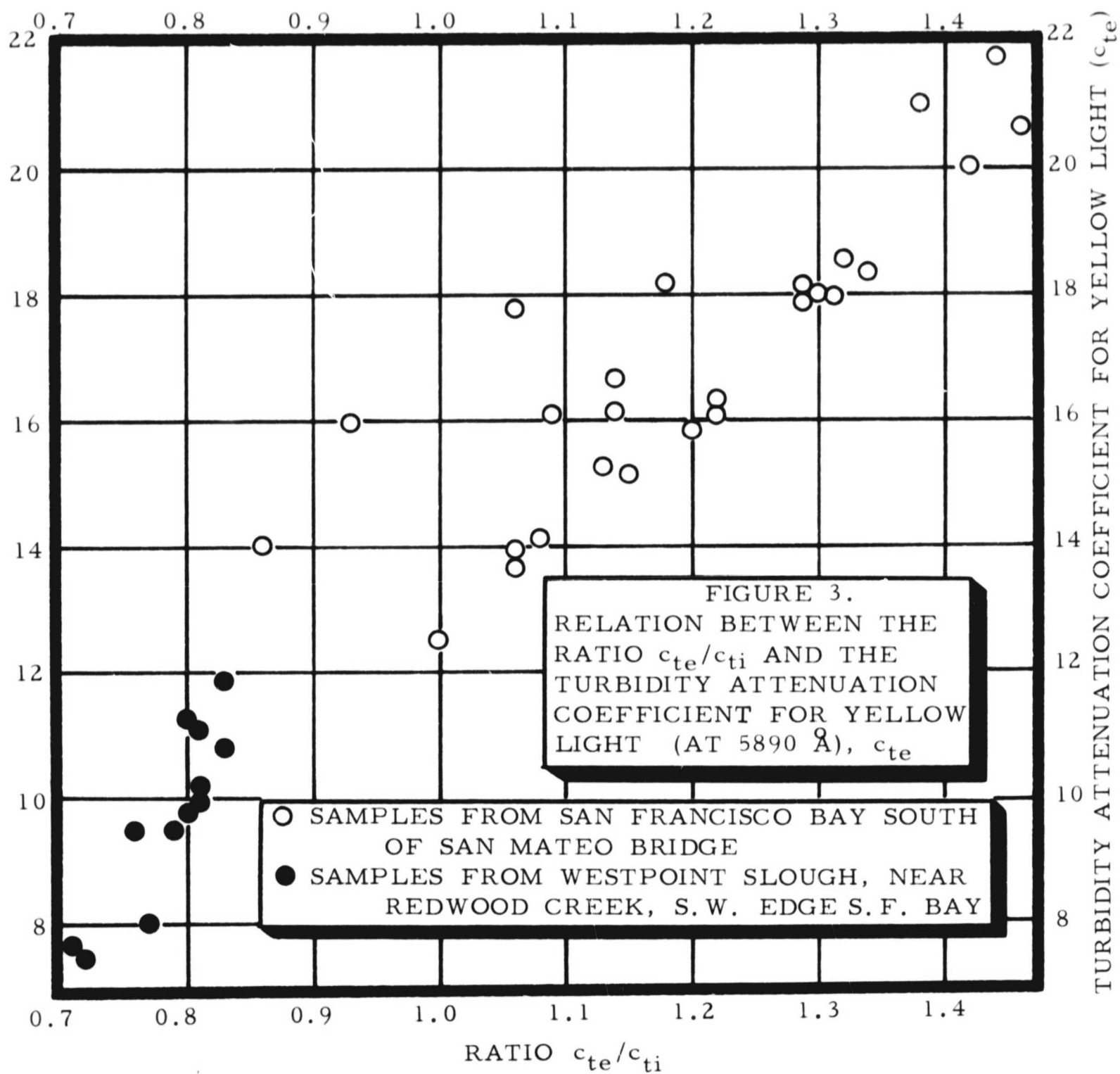


Table 5. Attenuation coefficients attributable to turbidity in San Francisco Bay and vicinity, showing relative consistence of the ratio c_{te}/c_{ti} *

| Samples from San Francisco Bay south of San Mateo Bridge (sampled from the ship POLARIS) | | | | Samples from Westpoint Slough, near Redwood Creek, southwest edge of S. F. Bay (from helicopter) | | | |
|--|--|--|------------------------------------|--|---|--|------------------------------------|
| (1) | (2) | (3) | (4) | (5) | (6) | (7) | (8) |
| Sample no. | $c_{te}(m^{-1})$ (Approx. turbidity attenua- tion coef- ficient for yel- low light) | $c_{ti}(m^{-1})$ (Approx. turbidity attenua- tion coef- ficient for inci- dent green sunlight) | Ratio: c_{te}/c_{ti} (2/3) | Sample no. | $c_{te}(m^{-1})$ (Approx. turbidity attenua- tion coef- ficient for yel- low light at 5890 Å) | $c_{ti}(m^{-1})$ (Approx. turbidity attenua- tion coef- ficient for inci- dent green sunlight) | Ratio: c_{te}/c_{ti} (6/7) |
| 188 | 15.1 | 13.2 | 1.15 | 87 | 11.2 | 14.1 | 0.80 |
| 192 | 13.9 | 13.1 | 1.06 | 89 | 10.8 | 13.0 | 0.83 |
| 201 | 13.6 | 12.8 | 1.06 | 92 | 8.0 | 10.3 | 0.77 |
| 207 | 18.5 | 14.1 | 1.32 | 96 | 10.2 | 12.6 | 0.81 |
| 208 | 16.1 | 14.8 | 1.09 | 98 | 11.1 | 13.6 | 0.81 |
| 209 | 12.5 | 12.6 | 1.00 | 100 | 7.6 | 10.7 | 0.71 |
| 217 | 18.1 | 14.0 | 1.29 | 103 | 9.5 | 11.9 | 0.79 |
| 218 | 16.1 | 13.2 | 1.22 | 104 | 10.0 | 12.3 | 0.81 |
| 219 | 16.3 | 13.3 | 1.22 | 105 | 11.8 | 14.3 | 0.83 |
| 220 | 15.8 | 13.1 | 1.20 | 108 | 5.1 | 6.4 | 0.79 |
| 221 | 16.1 | 14.1 | 1.14 | 109 | 7.4 | 10.3 | 0.72 |
| 222 | 14.1 | 13.0 | 1.08 | 112 | 5.6 | 9.0 | 0.62 |
| 235 | 16.6 | 14.6 | 1.14 | 115 | 9.8 | 12.2 | 0.80 |
| 239 | 17.9 | 13.9 | 1.29 | 116 | 9.5 | 12.4 | 0.76 |

* Attenuation coefficients were determined by an experimental apparatus, and the accuracy is unknown.

c_{te}/c_{ti} being less than 1.00 in approximately 5 out of 11 tested samples and greater than 1.00 in the remaining 6. The average value of the attenuation coefficient for yellow light (c_{te}) among these 11 samples was 0.77 m^{-1} while the average value for green light (c_{ti}) was 0.88 m^{-1} . These values seem anomalously high, being approximately double the values that would be expected from turbid coastal water (Polcyn and Rollin, 1969, Fig. 7; Stoertz, 1969b, Fig. 3). Because of the admittedly improvised and experimental nature of the attenuation apparatus the values must be considered preliminary. It is conceivable that turbidity attenuation coefficients were as high as 0.77 to 0.88 m^{-1} in the Bonita Channel west of Golden Gate, since the tests were less than 1 mile offshore, in an area close to the outflow of turbid water from San Francisco Bay, and in an area not known for particular clarity of water at that time of year. If the coastal waters were as turbid as indicated during the tests, the high sensitivity of the FLD to low dye concentrations is encouraging. In addition, this indicates the importance of sampling with depth in the less turbid ocean waters.

CALCULATION OF SENSITIVITY CORRECTION COEFFICIENTS

The necessity of one or more additional correction factors to permit rationalization of FLD records and interpretation of dye concentrations has been explained in a previous report (Stoertz, 1969). It was concluded that the principal factors still to be accounted for are luminescence efficiency of the rhodamine dye and instrumental sensitivity,

and that these are best compensated for by means of a single factor to be termed the sensitivity correction coefficient (S_c). This can be viewed as the increment in rho produced by the luminescence from an infinitely small quantity of a luminescent solute divided by that infinitely small quantity. Consequently it is a measure of the intrinsic luminosity of the dye and of instrumental sensitivity. Since the coefficient, as defined, contains indeterminate instrumental factors it is most useful to view it as an error factor, simply being the quantity necessary to balance the equation of calculated versus measured rho values after all known factors have been considered. If this quantity (S_c), when calculated for a number of rho values, shows some rational relationship to dye concentration, R (e.g., if $S_c \cong a R$, or if $S_c \cong a R^b$, etc.), then it can be inferred that most of the pertinent factors related to rho have been considered. It was further concluded that if the relationship can be expressed as a linear function (i.e., if $S_c \cong a R$), then the value "a" can be used in formulas estimating dye concentration (R) from FLD records (rho values).

Application of the above principles requires that every time the sensitivity correction coefficient is calculated in operational use of the FLD, the instrument must view rhodamine dye solutions of known concentration under sufficiently known conditions that all pertinent factors related to rho can be evaluated and included in a theoretical calculation of rho. It has been concluded (Stoertz and others, 1969) that this requirement will be best achieved by in-flight monitoring of standard

targets. The alternative was to actually sample the target area at frequent intervals in flight or from shipboard and to use these samples in approximately the same way that the standard targets are used. The principal requirement for this was that the rho value corresponding to the sample must be known or closely approximated. Because there is a mechanical problem of sampling precisely within the one-degree field-of-view of the FLD from the air, and similar problems of relating aircraft speed to sample location, the sensitivity coefficients are calculated for groups of samples. Then errors in sample locations may be compensating, permitting calculation of meaningful average values of sensitivity coefficients.

The method used in these calculations is illustrated by Table 6, a typical data-sheet covering samples #217 to #222, six of the samples that are also shown on Tables 1, 2, and 5. The formula for rho is a theoretical formula derived in a previous report (Stoertz, 1969b, equation #22). It assumes that vertical dispersal of the dye is nearly uniform throughout the column sensed by the FLD. Because of the very high turbidity of the water and the undoubted very low light penetration during this test, the assumption is probably valid.

The recorded rho values used as the basis of calculations in Table 6 (column #2) are the difference between the actual values recorded on the strip chart and the apparent "zero" value. The latter is taken as the average background level recorded when the FLD is viewing open water containing no dye, during level flight. This value varies during the tests

Table 6. Calculation of sensitivity correction coefficients of water samples from San Francisco Bay

(same samples as shown on Fig. 1, Fig. 2, Tables 1, 2, and 5; samples were obtained aboard POLARIS on May 20, 1969)

Formulas: $\rho = \frac{S_c t_c \sin \phi \csc \phi}{c_i \csc \phi + c_e}$ (or) $S_c = \frac{\rho(c_i \csc \phi + c_e)}{t_c \sin \phi \csc \phi}$

Assumption for trial purposes: $S_c \approx a R$ (in column # (22))

(-10 omitted after logs; figures were rounded after calculations completed.)

| 1 Sample no. | 217 | 218 | 219 | 220 | 221 | 222 |
|--|----------------|----------------|----------------|----------------|----------------|----------------|
| 2 Recorded ρ (ρ) | 0.065 | 0.085 | 0.375 | 0.225 | 0.025 | 0.045 |
| 3 ϕ (nearest 1°) | 68° | 68° | 68° | 68° | 68° | 69° |
| 4 ϕ (nearest $20'$) | $73^\circ 40'$ | $73^\circ 40'$ | $73^\circ 40'$ | $73^\circ 40'$ | $73^\circ 40'$ | $74^\circ 20'$ |
| 5 t_c | 0.99 | 0.99 | 0.99 | 0.99 | 0.99 | 0.99 |
| 6 c_i | 14.23 | 13.45 | 14.07 | 13.60 | 14.23 | 13.19 |
| 7 $\log \sin \phi$ | 9.967 | 9.967 | 9.967 | 9.967 | 9.967 | 9.970 |
| 8 $\log t_c$ | 9.996 | 9.996 | 9.996 | 9.996 | 9.996 | 9.996 |
| 9 $\log \csc \phi$ | 0.018 | 0.018 | 0.018 | 0.018 | 0.018 | 0.016 |
| 10 $\log c_i$ | 1.153 | 1.129 | 1.148 | 1.134 | 1.153 | 1.120 |
| 11 $\log(c_i \csc \phi) = (9) + (10)$ | 1.171 | 1.147 | 1.166 | 1.151 | 1.171 | 1.137 |
| 12 Antilog (11) | 14.83 | 14.02 | 14.66 | 14.17 | 14.83 | 13.70 |
| 13 c_e | 18.29 | 16.23 | 16.50 | 15.98 | 16.23 | 14.24 |
| 14 $(c_i \csc \phi + c_e) = (12) + (13)$ | 33.12 | 30.25 | 31.16 | 30.15 | 31.06 | 27.94 |
| 15 $\log \rho$ | 8.813 | 8.929 | 9.574 | 9.352 | 8.398 | 8.653 |
| 16 $\log(c_i \csc \phi + c_e) *$ | 1.520 | 1.481 | 1.494 | 1.479 | 1.492 | 1.446 |
| 17 $\log[\rho(c_i \csc \phi + c_e)] **$ | 0.333 | 0.410 | 1.068 | 0.831 | 9.890 | 0.099 |
| 18 $\log(t_c \sin \phi \csc \phi) ***$ | 9.981 | 9.981 | 9.981 | 9.981 | 9.981 | 9.982 |
| 19 $\log S_c = (17) - (18)$ | 0.352 | 0.429 | 1.087 | 0.851 | 9.909 | 0.117 |
| 20 $S_c = \text{Antilog } (19)$ | 2.251 | 2.688 | 12.22 | 7.092 | 0.812 | 1.310 |
| 21 R (ppb) | 12.5 | 14.2 | 45.4 | 27.2 | 5.2 | 7.2 |
| 22 $a \approx S_c / R \approx (20) / (21)$ | 0.180 | 0.189 | 0.269 | 0.261 | 0.156 | 0.182 |

* (16) = \log (14)

** (17) = (15) + (16)

*** (18) = (7) + (8) + (9)

and was almost invariably lower than the "zero" setting of the recorder pen. The level is probably related to differences in gain of the two photomultipliers. That such differences exist was previously demonstrated and is clearly evident on records made by artificial light (e.g., Fig. 1). This discrepancy is probably an inevitable consequence of using two photomultipliers and would be remedied in future designs of the FLD (D.A. Markle, ~~oral commun.~~, 1969).

The changes in operational "zero" level are not a problem because dye was confined to discrete patches and the aircraft crossed a non-luminescent water target before and after each pass across a dye patch. This made possible a frequent correction in compiling the data. In future operational tests this may be a problem if dye occurs throughout the water body. Then changes in zero level may be indistinguishable from changes in luminescence signal. The problem may be more serious over land because of continuous changes in reflectivity along a flight line. A possible solution is to include a non-luminescent target in the standard target device to give in-flight monitoring of operational zero level. A suitable material during tests on the ground, giving an FLD-reading similar to a tank of water, was a sheet of polished opaque black plastic (acrylic resin). This has the advantage that both the absolute reading and the noise level appeared similar to a calm, deep water target. The validity of this comparison has not yet been established by testing in flight over open water.

The values of sensitivity correction coefficient (S_c) calculated in Table 6 (column #20) need to consider dye concentration (R) in order to be used in calculation of dye concentration from rho values where water samples were not taken. To keep these calculations manageable, it is convenient to use a value that might be termed the sensitivity constant (a) in the relation (Stoertz, 1969b, equation #19):

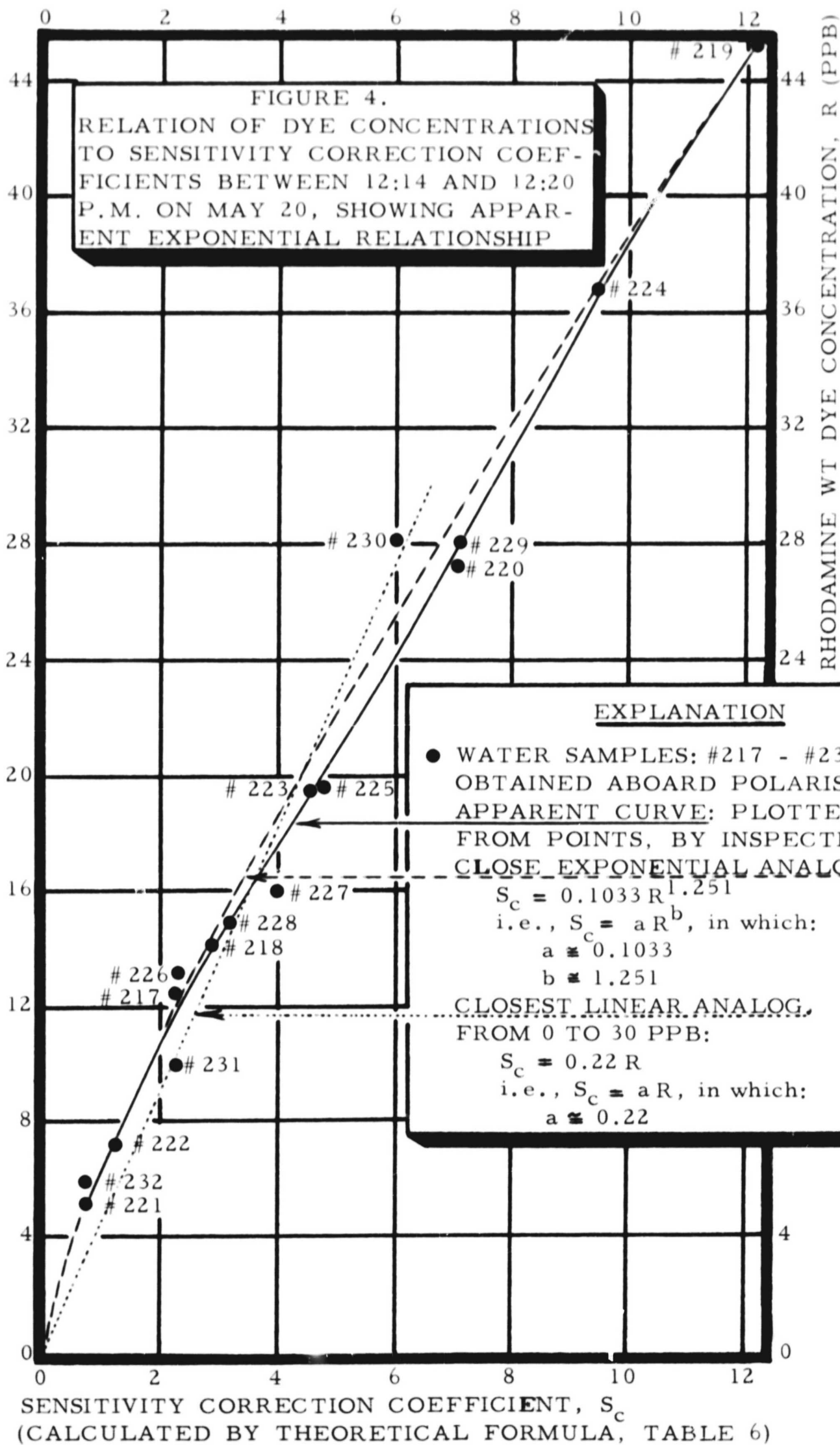
$$S_c \cong a R$$

Application of this equation using recent test data, as typified by Table 6 (columns #21 and #22), showed that average values of the "constant" (a) are a good approximation of (a) for short test periods. Comparison of a and R (Table 6) shows a residual proportionality, suggesting that a more accurate approximation is exponential:

$$S_c \cong a R^b$$

Verification that an exponential relation occurs for samples collected on May 20 is obtained graphically by plotting dye concentration (R) versus sensitivity correction coefficient (S_c , Fig. 4). Sixteen samples (#217 to #232) obtained between 12:14 and 12:20 p.m. are plotted on the graph. Determination of the approximate relation using the highest and lowest points (samples #219 and #221) is summarized in the following tabulation:

| <u>Samples</u> | <u>S_c values</u> | <u>R values</u> |
|----------------|--------------------------------|-----------------|
| #219 | 12.22 | 45.4 ppb |
| #221 | 0.812 | 5.2 ppb |



Assumed curve, for trial purposes:

$$S_c = a R^b$$

Substituting foregoing values in simultaneous equations:

$$12.22 = a 45.4^b$$

$$0.812 = a 5.2^b$$

taking logarithms:

$$\log 12.22 = \log a + b \log 45.4$$

$$\log 0.812 = \log a + b \log 5.2$$

Subtracting: $\log 12.22 - \log 0.812 = b \log 45.4 - b \log 5.2$

$$1.087 - (9.909 - 10) = b (1.657 - 0.716) \quad (\text{numbers are rounded})$$

$$b = \frac{1.087 + 0.0906}{1.657 - 0.716} = \frac{1.177}{0.941} = 1.251$$

solving for a:

$$12.22 = a 45.4^{1.251}$$

$$\log 12.22 = \log a + 1.251 \log 45.4$$

$$1.087 - 1.251 (1.657) = \log a$$

$$1.087 - 2.073 = \log a$$

$$\log a = -0.986$$

$$a = \text{antilog } (9.014 - 10) = 0.1033$$

resultant values: $a = 0.1033$

$$b = 1.251 \quad (\text{or}) \quad S_c \cong 0.1033 R^{1.251}$$

This curve is plotted on Figure 4 by dashed line. Alternatively, the closest linear approximation of the relation, but giving a greater error for the highest and lowest values, is:

$$S_c \cong 0.22 R \quad (\text{or}) \quad S_c \cong a R \quad \text{in which} \quad a \cong 0.22$$

This relation is given on Figure 4 by dotted line. The distribution of points is such that at concentrations less than 30 ppb either formula is suitable for an approximation. This illustrates that a linear approximation of the relation between dye concentration and sensitivity coefficient is generally sufficient relative to other assumptions that are made in compilation of the FLD data. In operational use, the errors may be minimal for field conditions that fit the low dye concentrations (e.g., 0 to 10 ppb); fortunately this is the range in most foreseeable studies.

Using similar procedures, the average values of the sensitivity constant (a) were calculated for segments of the test periods during which all factors appeared fairly constant. During future operational use it is envisioned that the length of such segments may be determined by the time interval between viewing standard targets. Practical limits may include such factors as variation in the illumination of the standard target device. The target may be shadowed on westbound traverses and illuminated on eastbound traverses.

RELATION OF SENSITIVITY TO SOLAR INTENSITY

A preliminary examination of FLD records from the recent airborne and shipboard tests in Menlo Park indicates a correlation occurs between low levels of solar intensity (component A) and FLD readings (rho). It is suspected that solar intensity variations might influence sensitivity of the instrument to increments in rhodamine dye. For this reason it is easier to use the ratio of dye concentration (R) to luminescence coefficient (rho)

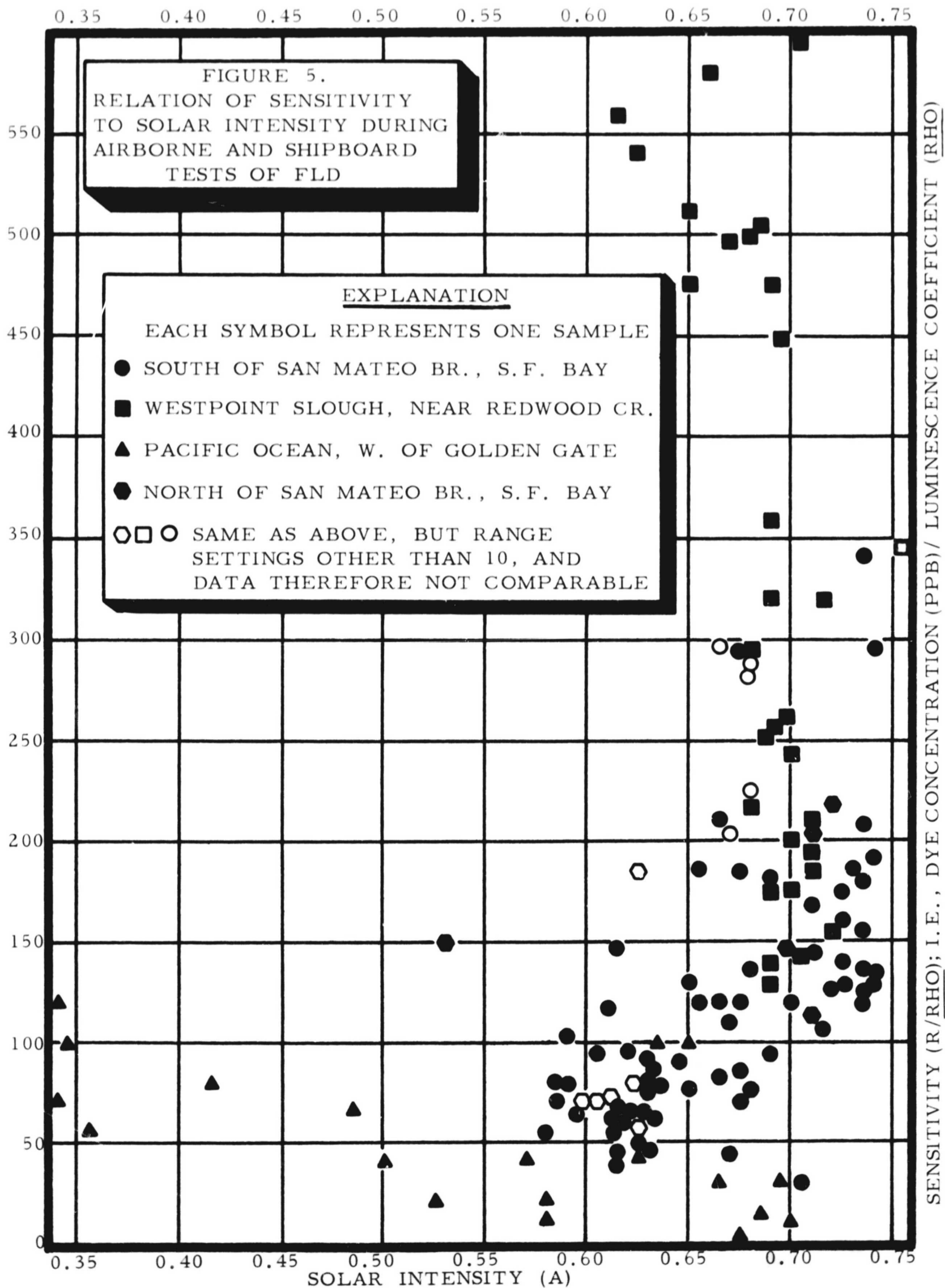
as a measure of sensitivity. A plot of these ratios (R/ρ) against solar intensity (A) is shown in Figure 5.

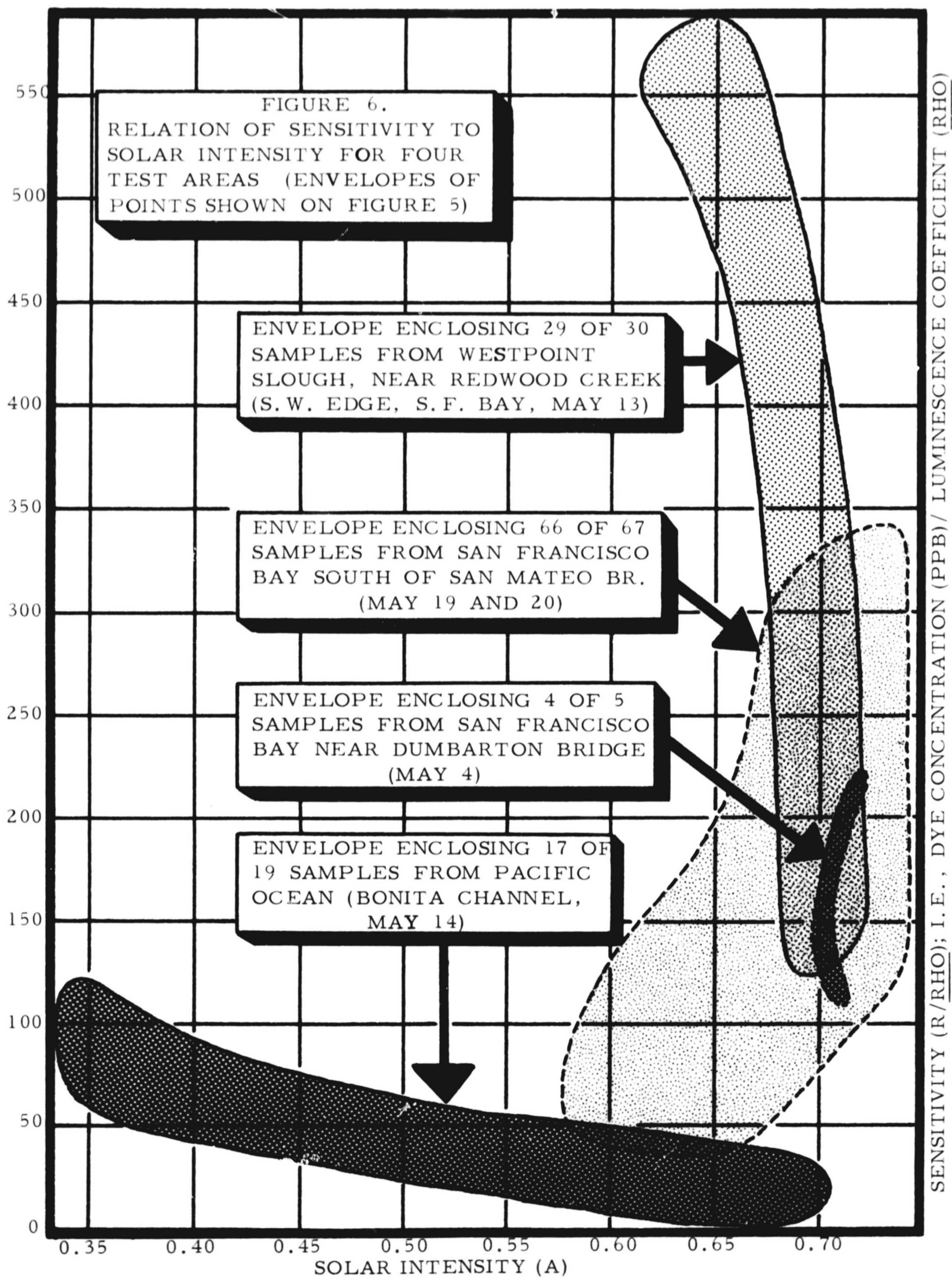
It is concluded from the graph that there is no correlation between sensitivity and solar intensity, but that there is less variation within each day of testing compared to different days. The samples from each test area cluster on the graph (Fig. 6). The variation with testing dates does not suggest that an instrumental drift with time could explain this distribution.

In general, no significant correlation is evident between sensitivity and solar intensity during the periods of sampling. These are the periods when the aircraft was flying nearly level over patches of rhodamine dye. Correlations between the two factors apparently occurred when the plane banked in turning at the ends of each traverse. Therefore, the records of solar intensity appear to be unnecessary in interpretation of dye concentrations from ρ values. It is useful to record A, however, since these fluctuations indicate movements of the plane.

RELATION OF FLD VALUES TO DYE CONCENTRATION

Data compilation is completed by dividing the test periods into segments of apparent uniformity of the principal variables described above. For example, the airborne and shipboard tests in Menlo Park from May 8 to May 20 were divided into 13 such segments averaging 10 minutes each. They ranged in length from 2 minutes to 21 minutes, and the instrument was re-calibrated during each segment using water





samples. An average of 10 water samples was used during each of the test segments, the number ranging from 5 to 16. Compilation is easier for longer segments, but less reliable. A principal factor in limiting the length is a change in apparent sensitivity of the instrument. This should be nearly eliminated in future models of the FLD by using only one photomultiplier (D.A. Markle, ~~oral commun.~~, 1969).

The method of calculating the relation between dye concentration (R) and FLD reading (rho) for a typical test segment is illustrated on Table 7. This utilizes the theoretical formula derived previously (Stoertz, 1969, equation #36), which assumes uniform dispersal of dye throughout the column sensed by the FLD. The calculation gives the average curve of dye concentration versus FLD reading that occurred during the test, by calculating rho values for four convenient points on the curve (values in column #23). The methods of calculating all unknowns in the formula (a , t_c , ϕ , c_{ti} , c_{wi} , c_{te} , c_{we} , h and f) have been described above.

The values substituted in Table 7 can be averages for all samples taken during the period or averages based either on time intervals between samples, linear distance between samples, or on frequency distribution of rho values represented by the samples.

A useful procedure for future operational use is to calculate the relation for dye concentrations less than 10 ppb, and use corresponding values of the variables. This would be important for variables having an exponential relation to dye concentration (viz., a , h , and f). In Table 7 the values were averages for all samples.

Table 7. Calculation of relation between dye concentration and FLD readings for selected short test period (12:14 to 12:20 p.m. on May 20, 1969)

Formula:
$$\rho = \frac{R a t_c \sin \phi \csc \theta}{R f \csc \theta + R h + c_{wi} \csc \theta + c_{ti} \csc \theta + c_{we} + c_{te}}$$

Notes: 1) Symbols are identified in accompanying text.

2) Columns #① to #②② are based on average values for the group of 16 samples identified in column #①.

3) Figures were rounded after calculations were completed.

4) (-10) is omitted from logarithms.

| ① | Samples | 217-232 | | | | | |
|---|---------------------------|-----------------|---|--------------------------------------|--------|----|------------------------------------|
| ② | a | 0.216 | ⑨ | $\log(c_{wi} + c_{ti})^*$ | 1.1149 | ①⑥ | $\log a = \log ②$ 9.3345 |
| ③ | t_c | 0.99 | ⑩ | $\log \csc \theta = \log ⑤$ | 0.0169 | ①⑦ | $\log t_c = \log ③$ 9.9956 |
| ④ | θ | $74^{\circ}10'$ | ⑪ | $\log [c_{wi} + c_{ti} \csc \theta]$ | 1.1318 | ①⑧ | $\log \sin \phi = \log ④$ 9.9692 |
| ⑤ | $\csc \theta$ | 1.0394 | ⑫ | Antilog ⑪ | 13.55 | ①⑨ | $\log \csc \theta = \log ⑤$ 0.0169 |
| ⑥ | $c_{ti} (m^{-1})$ | 12.98 | ⑬ | $c_{te} (m^{-1})$ | 15.87 | ②① | $①⑥ + ①⑦ + ①⑧ + ①⑨$ 9.3162 |
| ⑦ | $c_{wi} (m^{-1})$ | 0.05 | ⑭ | $c_{we} (m^{-1})$ | 0.14 | ②② | h 0.00064 |
| ⑧ | $c_{wi} + c_{ti} = ⑥ + ⑦$ | 13.03 | ⑮ | $⑫ + ⑬ + ⑭$ | 29.56 | | f 0.015 |

| ②③ | Selected R values (ppb) | ②③ | 1 | 10 | 20 | 40 |
|----|---|----|---------|--------|--------|--------|
| ②④ | $\log R = \log ②③$ | ②④ | 0.00 | 1.00 | 1.3010 | 1.6021 |
| ②⑤ | $\log \text{numerator} = ②① + ②④$ | ②⑤ | 9.3162 | 0.3162 | 0.6173 | 0.9183 |
| ②⑥ | $R h = ②③ \times ②①$ | ②⑥ | 0.00064 | 0.0064 | 0.0128 | 0.0256 |
| ②⑦ | $\log f = \log ②②$ | ②⑦ | 8.1761 | 8.1761 | 8.1761 | 8.1761 |
| ②⑧ | $\log(R f \csc \theta) = ①⑩ + ②④ + ②⑦$ | ②⑧ | 8.1930 | 9.1930 | 9.4940 | 9.7951 |
| ②⑨ | $R f \csc \theta = \text{Antilog } ②⑧$ | ②⑨ | 0.0156 | 0.1560 | 0.3119 | 0.6238 |
| ③① | $\text{Denominator} = ①⑮ + ②⑥ + ②⑨$ | ③① | 29.58 | 29.72 | 29.88 | 30.21 |
| ③② | $\log \text{denominator} = \log ③①$ | ③② | 1.4710 | 1.4731 | 1.4754 | 1.4802 |
| ③③ | $\log \rho(\text{rho}) = ②⑤ - ③②$ | ③③ | 7.8452 | 8.8432 | 9.1419 | 9.4381 |
| ③④ | $\rho(\text{rho}) = \text{Antilog } ③③$ | ③④ | 0.0070 | 0.0697 | 0.1386 | 0.2742 |

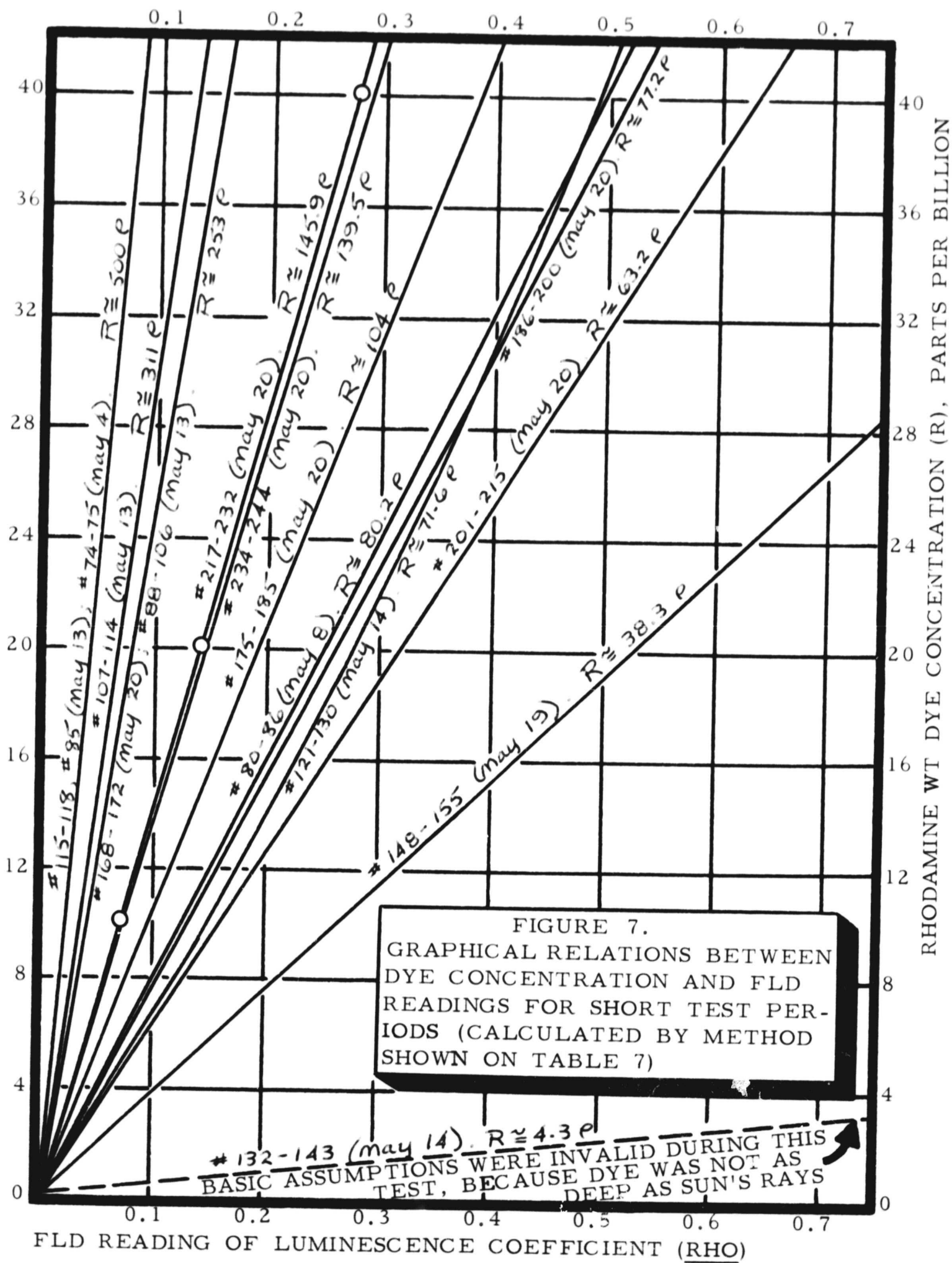
* ⑨ = $\log ⑧$
 ⑩ = $\log ⑤$
 ⑪ = ⑨ + ⑩

The actual curve of R versus rho can be plotted, or the relation can be treated mathematically. The curve delineated by Table 7 is shown on Figure 7 (solid line). Curves calculated for other test segments are plotted on the same graph (dashed lines). Most of the relations are nearly linear, and the linear analog of each curve is shown (Fig. 7).

These curves are used in scaling the strip-chart records to read directly in terms of dye concentration. A typical FLD record showing the final scaling (horizontal ruled lines) is illustrated in Figure 8.

A segment of strip-chart record during a period of significantly lower sensitivity is illustrated by Figure 9, made during tests over Westpoint Slough, near Redwood Creek. A period of significantly higher sensitivity is illustrated by Figure 10, made during tests over San Francisco Bay north of San Mateo Bridge. The latter record also illustrates sufficiently rapid chart speed (1 inch per second) to show the limitations of pen response time. The uniform slope of all peaks apparently results from this limiting factor. A comparison of the spacing of horizontal lines on Figures 8, 9, and 10 shows that changes in sensitivity are appreciable.

A period of high sensitivity is illustrated by Figure 11, made during tests over the Pacific Ocean west of Golden Gate. The high sensitivity is attributable to the clarity of the water and possibly to the dispersal of dye with depth. The FLD readings could not be interpreted by formula because sampling with depth was not done and because the



vertical column of water sensed by the FLD was probably much deeper than the lower limit of the dye. Surface samples (#142 and #143) analyzed by a laboratory fluorometer showed concentrations of 0.5 and 1.4 ppb. Locations of these samples as shown on Figure 11 are at the lowest possible levels of rho. This indicates a sensitivity of 0.1 or 0.2 ppb was achieved.

SUMMARY AND CONCLUSIONS

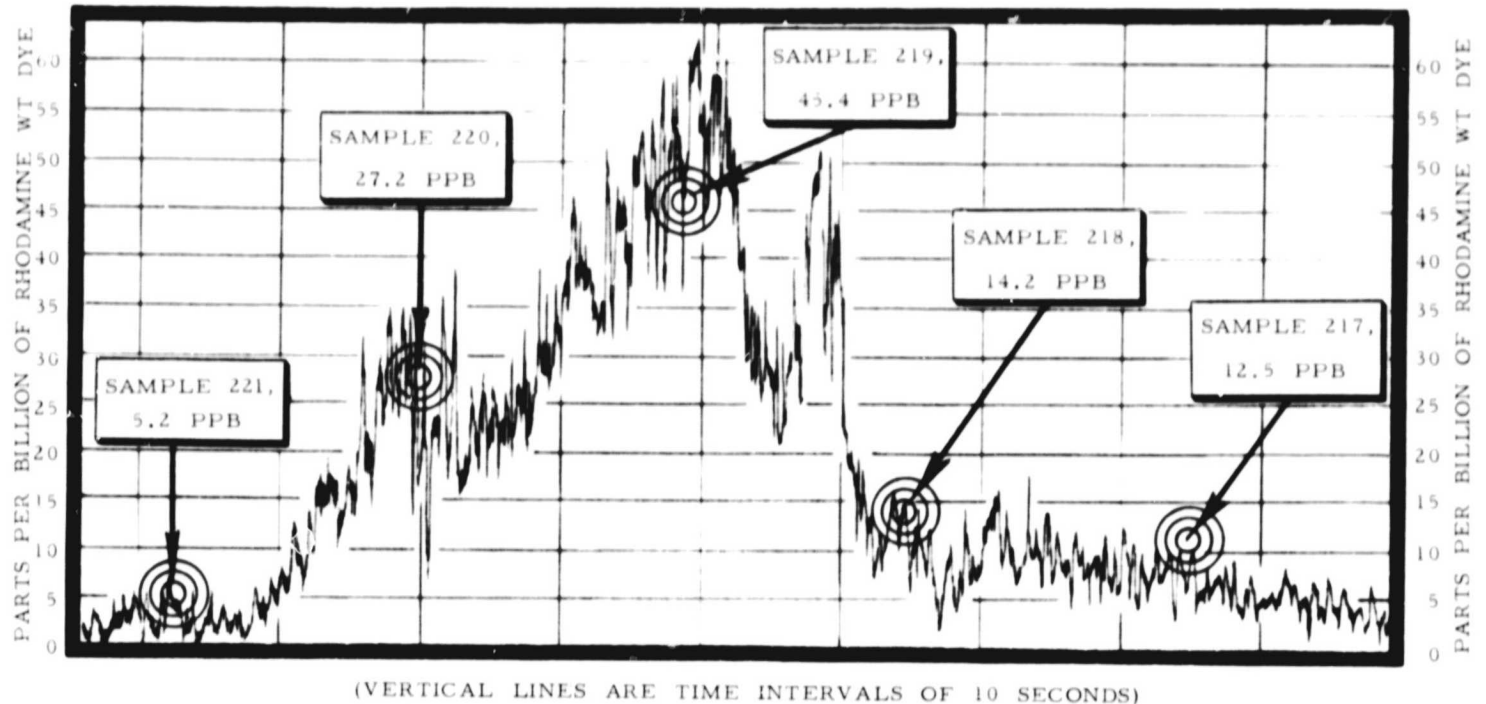
1) Several environmental factors related to function of the FLD over open water are water turbidity, water temperature, and fluorescent dye concentration. Consequently, variations in depth of light penetration, attenuation of emitted luminescence, and attenuation of incident sunlight occur continuously in space and time. Sun angle and instrumental sensitivity vary in a less complicated way.

2) Methods of estimating the above factors and of compiling the resulting data have been tested. The methods approximate those to be used in future operational use.

3) Using an artificial light source in which components A and B are equal, there is a large error between recorded values of components A and B. This will not be a problem for an FLD having only one photomultiplier.

4) Laboratory work with attenuation equipment indicates that absorption or attenuation of yellow light by Rhodamine WT dye is very slight relative to other factors. Therefore, in natural water samples, self-absorption of luminescence by dye appears to be negligible when compared to absorption by the suspended particles.

RECORD FROM FLD USED AS SHIPBOARD FLUOROMETER, S.F. BAY, MAY 20, 1969



Explanation

Record made aboard POLARIS during passage across a cloud of rhodamine dye of concentrations ranging from 2 ppb to 60 ppb.

Recorder pen line is a trace of luninescence coefficient (rho) computed by the analog computer in the FLD.

Period shown is from 12:13 p.m. plus 50 seconds to 12:15 p.m. plus 25 sec.

Horizontal lines are dye concentrations for average conditions during the 95-second period shown, calculated by the theoretical formula:

$$R = \frac{\rho(c_{wi} \csc \theta + c_{ti} \csc \theta + c_{we} + c_{te})}{a t_c \sin \phi \csc \theta - f \rho \csc \theta - h \rho}$$

Close empirical analog of sensitivity: $\rho = 0.007042 R$

Location: latitude $37^{\circ}34'N.$, longitude $122^{\circ}12'W.$

Sun angle above horizon: approx. 68° at right edge, slightly higher at left.

Water temperature: $20.2^{\circ}C.$

Temperature correction coefficient: 0.99

General location: South of San Mateo Bridge.

Figure 8. Record from Fraunhofer Line Discriminator used as a shipboard fluorometer in San Francisco Bay, May 20, 1969

5) Absorption of green light by Rhodamine WT dye appears to be more significant than is the case for yellow light. Absorption of such light by suspended particles in the turbid waters of San Francisco Bay is many times greater than that of a 100-ppb dye solution.

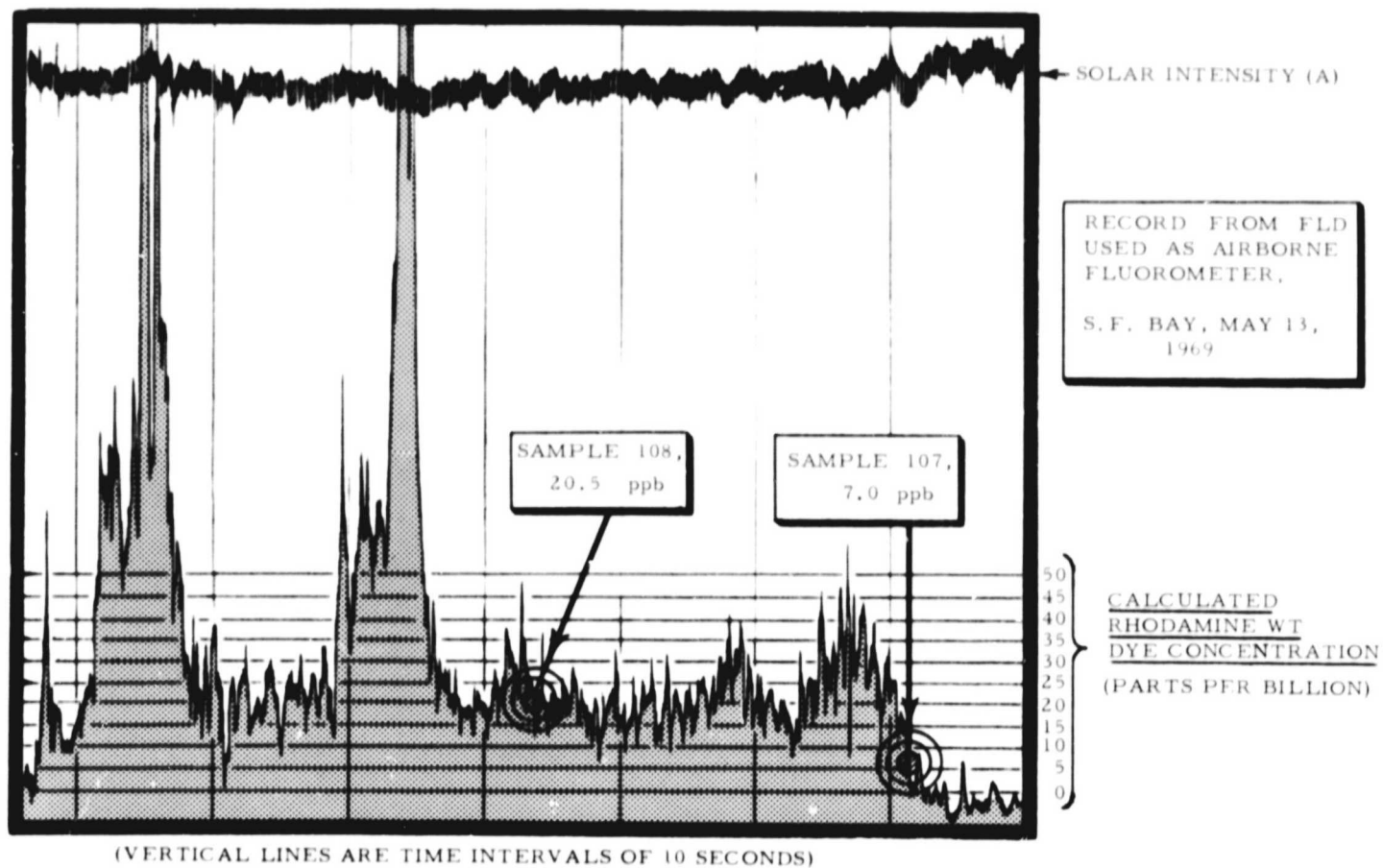
6) If coastal waters used for FLD tests are as turbid as indicated by measurements, then the observed high sensitivity of the FLD to low dye concentrations is very encouraging. This finding also indicates the necessity of sampling subsurface waters during use of the FLD. A limitation of the present method is the assumption that the dye is uniform throughout the water column sensed by the FLD.

7) Attenuation from dissolved dye in water samples has been calculated and expressed as a function of dye concentration. These relations are such that the constants f and h are evaluated as approximately equal to 0.015 m^{-1} and 0.00064 m^{-1} respectively.

8) An assumption required without use of a computer, is that there are linear relations between the dye concentration and sensitivity, emitted light attenuation, and incident light attenuation.

9) Limitations in the experimental attenuation equipment made estimation necessary of attenuation coefficients of pure water for yellow light (5890 Å) and for green light, from published data (Jerlov, 1968; Polcyn, and Rohlin, 1969). ~~B.A. 1969~~.

10) A limitation is that attenuation coefficients due to suspended particles and to dissolved dye were measured by the same experimental equipment and need further scrutiny.



Explanation

Record was made from H-19 helicopter during passage over a patch of rhodamine dye of concentrations ranging from 0 to approximately 250 parts per billion.

Upper record is a trace of solar intensity as monitored through upper portal of the FLD (component A).

Lower record is a trace of luminescence coefficient (ρ) as computed by analog computer using data from both portals. Horizontal lines are dye concentrations calculated by means of theoretical formula, as on Figure 8.

Close empirical analog of sensitivity: $\rho = 0.003215 R$

Location: latitude $37^{\circ}31'N.$, longitude $122^{\circ}12'W.$

Sun angle above horizon: approx. 70° .

Water temperature: $17.8^{\circ}C.$

Temperature correction coefficient: 1.06

Figure 9. Record from Fraunhofer Line Discriminator (FLD) used as an airborne fluorometer over Westpoint Slough, near Redwood Creek, southwest edge of San Francisco Bay, May 13, 1969.

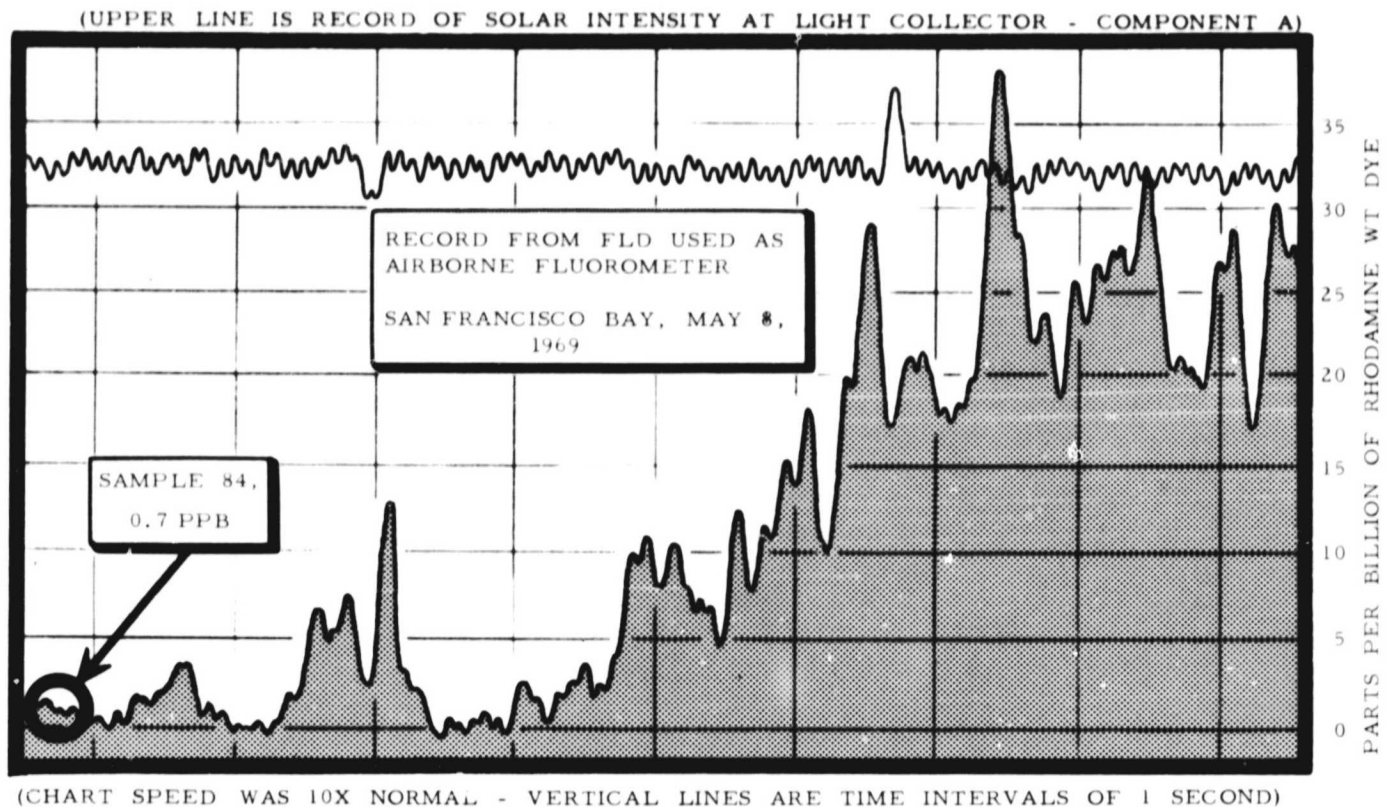
11) During test periods, the relative attenuation of yellow light and of green light by suspended particles is nearly a constant. This ratio is characteristic of the water at the time and place of testing. Consequently, one determination of the attenuation coefficient may be adequate for a given sample area.

12) Mechanical problems of sampling within the one-degree field-of-view of the FLD from the air, and of determining sample location mean that, presently, single samples would be difficult to evaluate. Groups of samples are averaged in calculation of sensitivity coefficients, thereby reducing the magnitude of probable error.

13) An exponential relation probably occurs between dye concentrations and sensitivity coefficients. However, the curve of this function approaches a linear approximation. This approximation makes compilation of test data easier.

14) There is no significant correlation between sensitivity and solar intensity during periods of level flight. Presently, records of solar intensity (A or B) are not necessary in interpretation of dye concentration from rho values. Such correlations were significant during banking of the aircraft, however, and may limit calculations to periods of level flight.

15) The average duration of test period resolved as a discrete segment in calculation of dye concentrations is 10 minutes. During such periods all factors except dye concentration can be represented by constant values.



Explanation

Record made from H-19 helicopter during passage over the margin of a patch of Rhodamine WT dye in San Francisco Bay.

Strip chart speed was sufficiently rapid (1 inch per second) to show effect of slow pen response time, resulting in uniform slopes.

Horizontal lines show dye concentrations calculated by theoretical formula, as on Figure 8.

Location: latitude $37^{\circ}40'N.$, longitude $122^{\circ}15'W.$

Sun angle above horizon: 64°

Water temperature: $17^{\circ}C.$

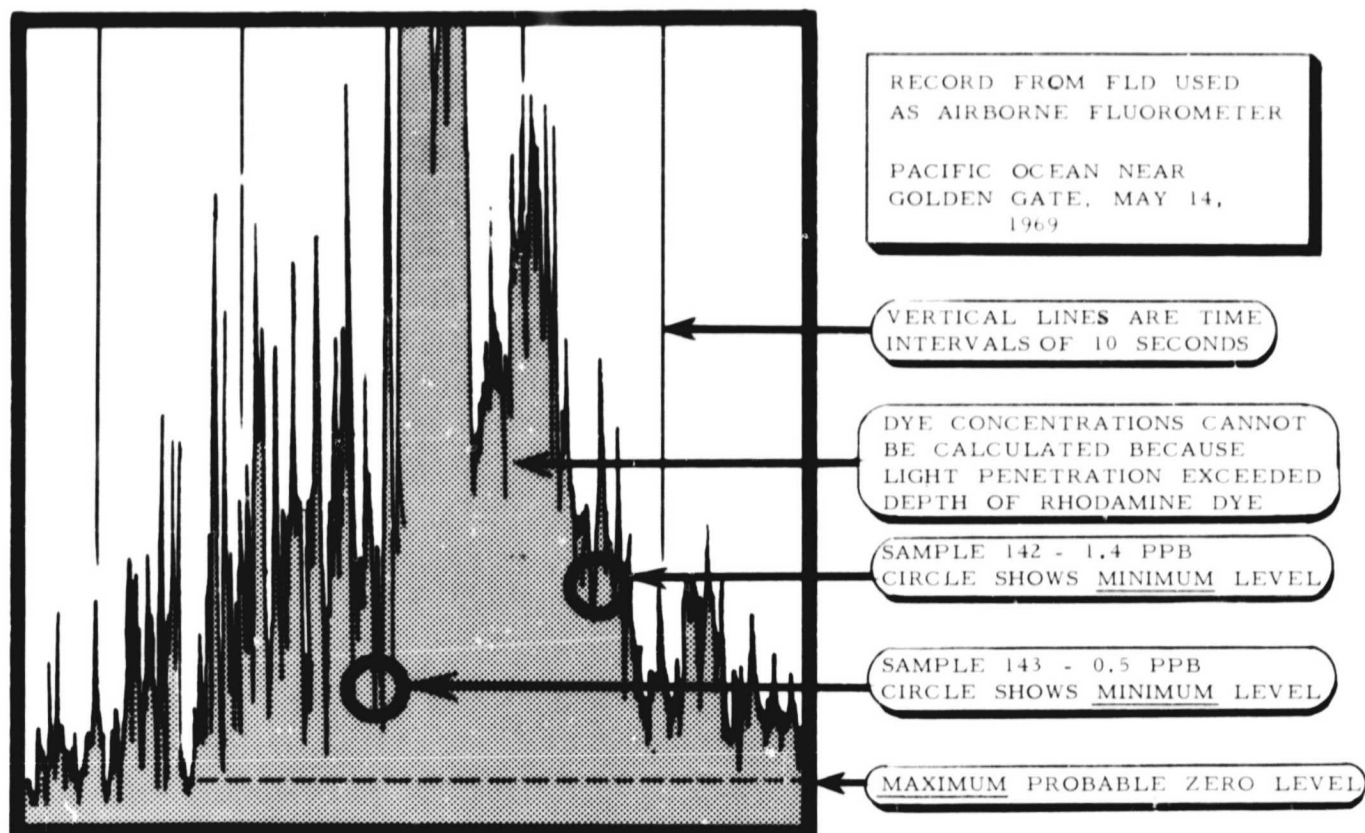
Temperature correction coefficient: 1.08

Figure 10. Record from Fraunhofer Line Discriminator (FLD) used as an airborne fluorometer over San Francisco Bay, May 8, 1969.

16) Exceptionally high sensitivity occurred during tests over the Pacific Ocean west of Golden Gate, as a result of relatively clear water. In areas of well dispersed dye the sensitivity appeared to differentiate increments as small as 1 or 2 tenths of one part per billion. Sampling with depth will be required to verify this.

17) A computer is needed for compilation of larger quantities of FLD data, and a future FLD should produce digital output.

18) A comparison of FLD records shows that significant changes in sensitivity occurred and illustrates the necessity of repeated calibration. A new design for the FLD, having only one photomultiplier, should essentially eliminate problems of varying sensitivity (Markle, D.A., ~~oral commun.~~, 1969). 1969).



Explanation

Record made from H-19 helicopter during passage over a highly dilute patch of well-dispersed dye in relatively clear water. Dye concentrations cannot be accurately calculated by theoretical formula because light penetration exceeded depth of the dye. Graph shows extremely high sensitivity to small dye increments, due to clarity of water and considerable dispersal of the dye with depth.

Period shown is from 1:30 p.m. plus 40 seconds to 1:31 p.m. plus 35 seconds; time progresses from right to left.

Figure 11. Record from Fraunhofer Line Discriminator used as an airborne fluorometer over Pacific Ocean west of Golden Gate, May 14

REFERENCES CITED

- Jerlov, N. G., 1968, Optical Oceanography: Elsevier Publishing Co., New York
- Nevin, C. M., 1949, Principles of structural geology: John Wiley and Sons, Inc., New York, p. 380
- Polcyn, F. C. and Rollin, R. A., 1969, Remote sensing techniques for the location and measurement of shallow-water features: Willow Run Laboratories, Univ. of Michigan, 8973-10-P.
- Stoertz, G. E., 1969, Fraunhofer line-depth sensing applied to water: U. S. Geol. Survey Open File Report
- Stoertz, G. E., Hemphill, W. R., and Markle, D. A., 1969, Airborne fluorometer applicable to marine and estuarine studies: Marine Technology Society Journal, v. 3, no. 6, p.
- Strahler, A. N., 1962, Physical geography: John Wiley and Sons, Inc., New York, p. 88
- U. S. Naval Observatory, 1967, The American Ephemeris and Nautical Almanac for the year 1969: U. S. Government Printing Office, Washington, D. C., 526 p.